

## UPPER CRUSTAL STRUCTURE, LIVERMORE VALLEY AND VICINITY, CALIFORNIA COAST RANGES

BY ANNE S. MELTZER, ALAN R. LEVANDER, AND WALTER D. MOONEY

### ABSTRACT

**We have interpreted two reversed seismic refraction profiles in the Livermore Valley area of California using travel times and amplitudes calculated with asymptotic ray theory. The upper crustal structure to 5 km depth is different on either side of the Greenville fault zone. The fault does not appear to extend below 5 km. The fault zone disrupts arrivals of rays which turn in the fault zone, but does not appear to affect rays that turn below 5 km. East of the Greenville fault zone, the boundary between the Cretaceous Great Valley sequence and Franciscan assemblage rocks occurs along a north-dipping interface below 4.5 km depth. West of the Greenville fault, the boundary between valley fill sediments and Franciscan rocks was not observed. Miocene sediment having a high compressional velocity, 5.0 km/sec, is present beneath Livermore Valley to at least 5 km depth. In contrast, the maximum velocity associated with adjacent Cretaceous sediments is 4.2 km/sec. The high velocity of the Livermore basin sediments seen in the refraction data is also observed on sonic logs made in exploratory wells in the basin which bottom in Miocene sediments. This last finding is important, since velocities of 4.8 to 5.0 km/sec have previously been associated with shallow Franciscan rocks. This observation calls into question the use of seismic velocities to distinguish between different Coast Range-Great Valley lithologies without other corroborating data.**

### INTRODUCTION

Livermore Valley of central California is to the east of Berkeley and south of Mount Diablo in the Coast Ranges (Figure 1). It lies above the older and more extensive Livermore basin. The dominant rock types exposed at the surface in the Livermore area are: the graywackes and basic intrusive rocks of the Franciscan assemblage accretionary complex; Cretaceous forearc basin sediments of the Great Valley sequence; and Tertiary sediments associated with Neogene basin formation (Figure 1). The basin is bounded on the west and east by two active right-lateral strike-slip faults, the Calaveras and Greenville faults, respectively. The present day structural basin is bounded on the north and south by anticlinal uplifts of the Franciscan assemblage which form Mt. Diablo and the central Diablo Range (Figure 1).

Following an earthquake along the northern part of the Greenville fault in January 1980, the U.S. Geological Survey shot two short reversed refraction profiles. The refraction profiles were acquired to better define the compressional wave velocity structure of the upper crust in order to improve the location of shallow earthquakes. The first profile is a 52 km NW-SE trending strike profile. Average station spacing over the length of the line is 0.85 km. This line is east of and approximately parallel to the Greenville fault (Figure 2). The second profile extends 70 km in a WNW-ESE direction, crossing the regional structural strike approximately perpendicularly. It crosses the Calaveras fault in the west, passes through the Livermore Valley, and then crosses the Greenville fault in the east. Average station spacing along the length of the dip profile is 1.23 km. Two shots were fired on each profile. In this

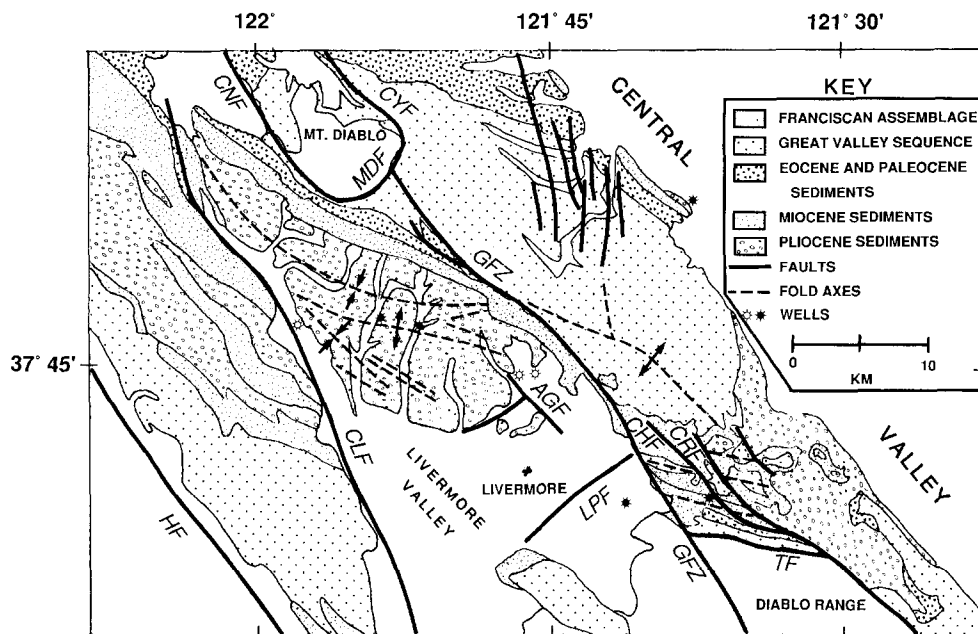


FIG. 1. Geologic map of Livermore Valley and vicinity. Major faults in the area include: HF = Hayward fault; CLF = Calaveras fault; CNF = Concord fault; MDF = Mt. Diablo fault; CYF = Clayton fault; GFZ = Greenville fault zone; AGF = Ancestral Greenville fault; LPF = Los Positas fault; CHF = Corral Hollow fault; CRF = Carnegie fault; and TF = Tesla fault (after Dibblee and Darrow, 1981). Major fold axes and locations of wells discussed in the paper are shown on the map. Closed well symbols indicate wells for which sonic logs were available.

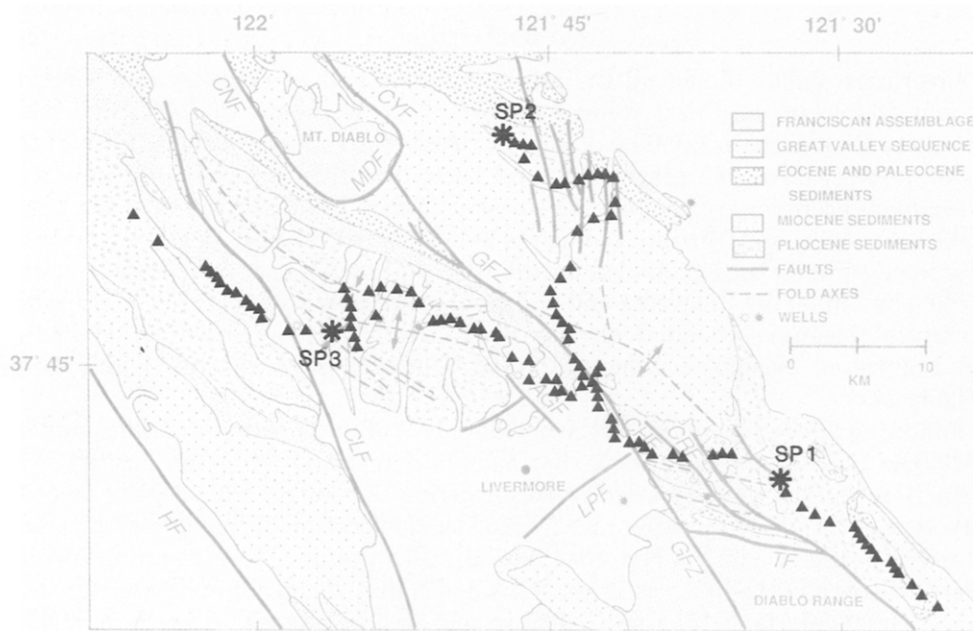


FIG. 2. Station location map for the strike and dip profiles. Receivers were laid out along roads in the area and follow a sinuous path. SP 2 is located in the north, SP 3 in the west, and SP 1 in the southeast. SP 1 and the receivers southeast of the Greenville fault are the same for both profiles. Receivers along both profiles are located within the Greenville fault zone. Abbreviations are the same as in Figure 1.

paper, we discuss the velocity models derived from analysis of the refraction profiles and their relation to the known geology.

### GEOLOGIC SETTING

The Livermore Valley area experienced complex tectonic evolution as the California margin underwent transition from a convergent to a transform plate boundary (Atwater, 1970). The valley, trending transverse to the dominant NW-SE structural grain found east of San Francisco, sits above the more extensive Neogene Livermore basin. The basin is bounded on all sides by major structural features. The western boundary of the basin is the right-lateral Calaveras fault which separates the Livermore basin from the East Bay Hills structural domain to the west (Aydin and Page, 1984). The present-day eastern boundary of the basin is the active Greenville fault system, a major NW-striking zone of faults extending 90 km southeast from Mt. Diablo. This fault system has at least 9 km of accumulated right-lateral offset (Carpenter *et al.*, 1984). The other major structural features bounding the basin are the uplifted Franciscan and ultramafic rocks which form the core of Mt. Diablo to the north and the central Diablo Range to the south. Mt. Diablo has been thrust up along the north-dipping Mt. Diablo fault, upending, and partially overturning Tertiary sediments of the Livermore basin, and causing a series of folds to form within the basin (Figure 1). Extensive outcrops of Franciscan rocks form the Diablo Range, an uplifted doubly plunging anticline.

The oldest rocks exposed on the surface in the area of this study are the Jurassic and Cretaceous coeval Franciscan assemblage and Great Valley sequence. The Franciscan assemblage consists of graywacke, shale, and lenses of chert and greenstone (Bailey *et al.*, 1964). These rocks have undergone low-grade, low-temperature, high pressure metamorphism and have been extensively deformed. Closely associated with these rocks are intrusive ultramafic serpentinites and diabase. This entire rock assemblage is interpreted as remnants of a subduction complex associated with Mesozoic and early Tertiary subduction along the western margin of North America (Ernst, 1970). The Great Valley sequence is a series of micaceous shales and arkosic turbidite sandstones that were deposited in a forearc basin east of the Franciscan accretionary complex (Dickinson, 1976; Ingersoll, 1982). The Great Valley sequence is believed to have been deposited on a trapped slab of oceanic crust (Dickinson and Seely, 1979). Cretaceous rocks are found in extensive outcrops forming a broad anticline east of the Greenville fault zone (Figure 1).

The original contact between the accretionary prism and forearc basin rocks has been mapped as the Coast Range Thrust (Page, 1966; Bailey *et al.*, 1970). Mafic and ultramafic rocks interpreted as uplifted ophiolite from the base of the Great Valley sequence are often found associated with the Coast Range thrust. These rocks are most commonly observed as metagabbros and serpentinites believed to be altered fragments of oceanic crust and upper mantle. Both the Franciscan assemblage and Great Valley sequence represent widespread regional deposits. These deposits underlay the Livermore basin, but their distribution at depth is not well known.

The original contact between the Franciscan and Great Valley rocks has been obscured in this area by Neogene wrench fault tectonics associated with dextral shear between the North American and Pacific plates (Atwater and Molnar, 1973; Dickinson and Snyder, 1979). The exposed contact between Franciscan and Great Valley sequence rocks in this area occurs along faults at the base of Mt. Diablo in the north, and along the Tesla fault to the SE. Exploratory wells drilled in the

Livermore Oil Field immediately west of the Greenville fault have penetrated both Cretaceous and Franciscan rocks at depths of 600 to 900 m (2,000 to 3,000 ft). This locally constrains the Franciscan-Great Valley contact beneath Livermore basin and led to the proposal of an ancestral Greenville fault now buried beneath the valley sediments (Sweeney, 1982). Other faults in the vicinity of Livermore include the Corral Hollow and Carnegie faults. These faults show minor dextral offsets of fold axes in Cretaceous and Tertiary sediments.

The Tertiary Livermore basin fill is exposed along the southwest flank of Mt. Diablo. Up to 850 m (2,800 ft) of middle Eocene marine shales and sandstones rest unconformably above the Cretaceous Great Valley sequence (COSUNA, 1984). During the Miocene, Livermore basin became a discrete depositional basin (Springer, 1983). Exploratory wells in Livermore Valley have penetrated more than 1,500 m (5,000 ft) of Miocene shallow marine to nonmarine siltstones, sandstones, and mudstones resting unconformably above the lower Tertiary rocks. Up to 4,500 m (15,000 ft) of nonmarine-interbedded Pliocene conglomerates, sandstones, and mudstones were deposited above the Miocene sediments. The Neogene sediments exhibit rapid lateral facies changes and basinward thickening indicative of structural growth and syntectonic deposition of sediments during this time. Deposition of the Miocene/Pliocene sediments records filling of a rapidly subsiding, tectonically active basin (Springer, 1983).

The Neogene tectonic setting and basin evolution of the Livermore basin are characteristic of wrench fault basins formed within right-stepping right-lateral strike-slip fault systems (Crowell, 1974; Rodgers, 1980; Aydin and Page, 1984). The time of maximum basin subsidence and a shift from predominantly marine to nonmarine deposition correspond in time to the approach and passage of the Mendocino triple junction at the latitude of Livermore, about 6 m.y. B. P. (Dickinson and Snyder, 1979). Northward migration of the triple junction marks the onset of the transform margin and wrench fault tectonics resulting in local compression, extension, and formation of local sedimentary basins (Blake *et al.*, 1978; Graham *et al.*, 1984). Early extension appears to have been followed by compression. A shift in plate motions 4.5 m.y. ago (Minster and Jordan, 1978; Page and Engebretson, 1984) could have resulted in a change in relative motion along a series of active faults, resulting in transpression and uplift in the Pliocene (Page, 1981; Springer, 1983). The entire Livermore structural domain is still tectonically active today as evidenced by continued uplift of Mt. Diablo, subsidence in the valley, and recent seismicity (Ellsworth and Marks, 1980). From the refraction seismologist's point of view, the basin is structurally complex, with numerous small features oblique or normal to regional trends.

#### DATA

The U.S. Geological Survey shot two reversed seismic refraction profiles in the Livermore basin area. We have interpreted each line using iterative two-dimensional raytracing techniques based on asymptotic ray theory (Červený *et al.*, 1977), modeling both travel times and amplitudes. Travel times were fit to within 0.05 sec. Synthetic records were produced to model amplitudes using the algorithm of McMechan and Mooney (1980). The field records and synthetic seismograms shown in this paper are plotted in true relative amplitude and are plotted by absolute distance from shot to receiver (Figure 3).

We have modeled the refraction data as though they were recorded along straight profiles, although the necessity of laying receivers out along roads resulted in

## SHOTPOINT 1 STRIKE LINE

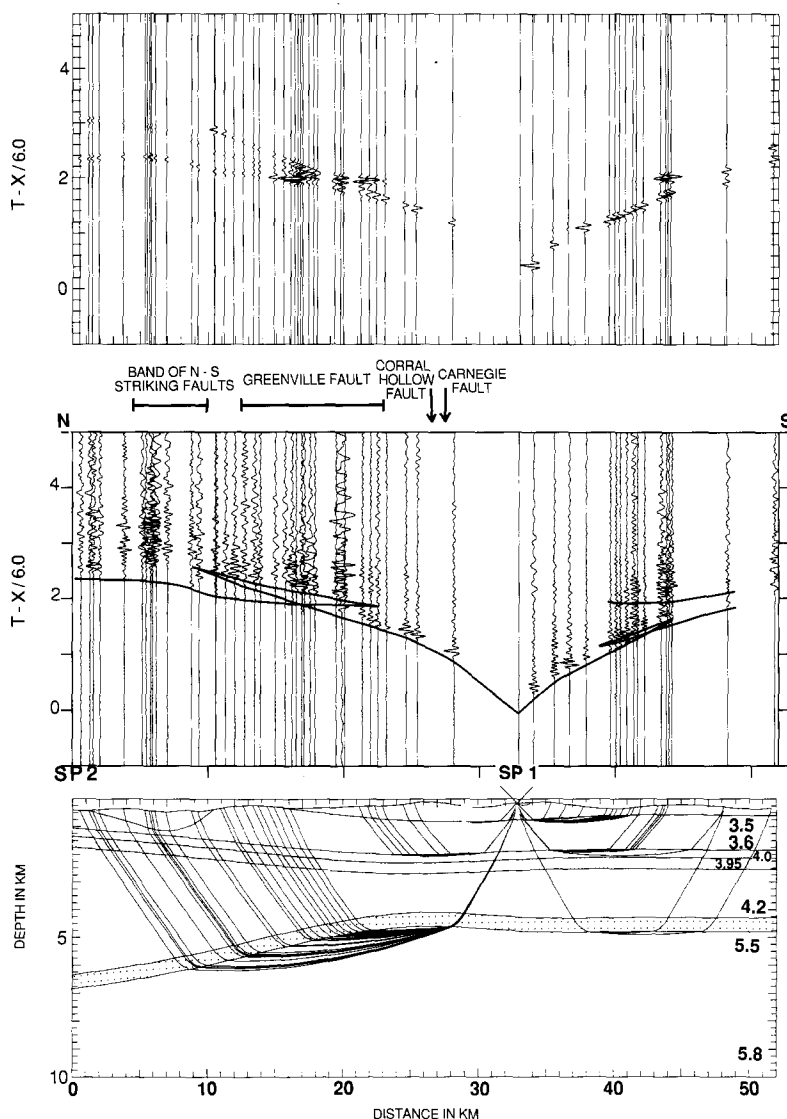


FIG. 3. Data from SP 1 strike profile. Raytrace model with first arrivals is plotted below the data. Travel-time curves from the raytracing are superimposed on the data. The synthetic seismograms from the model are plotted above the data. Intersection of major faults with the receivers is shown directly above the data. The profile cuts obliquely through a band of north-south striking faults at 2 to 10 km and runs parallel to part of the Greenville fault. A velocity of 2.1 km/sec was assumed for the shallow wedge-shaped feature associated with the north-south striking band of faults. The other surface layer that extends from 15 to 52 km in the model has velocities which increase from 2.1 to 3.0 km/sec. The shaded layer within the 4.0 to 4.2 km/sec layer is a mild velocity inversion with velocities of 3.95 to 4.0 km/sec. A velocity gradient zone between the 4.0 to 4.2 and 5.5 to 5.8 km/sec layers is indicated by the dotted layer.

crooked line geometries, introducing some degree of three-dimensionality into the data. The shot and station spacing density are insufficient to model these profiles as a three-dimensional data set. We feel the closeness of the travel-time and amplitude modeling to the recorded data indicates that using a two-dimensional model satisfactorily approximates the three-dimensional recording geometry. The two profiles are roughly parallel to the regional structural strike and dip, and we

have designated them as strike and dip profiles in the text. Distances along the profiles are referenced in both the text and figures from the north and east end of each line, respectively. As discussed more fully later, the dip profile actually crosses a number of structures, some in a dip direction and some in a more nearly a strike direction.

*Strike profile.* The strike profile is a 52 km NW-SE trending profile located east of and parallel to the Greenville fault zone (Figure 2). Two shots, 33 km apart, were located along the profile: one at shotpoint 1 (SP 1) in the south and the other at shotpoint 2 (SP 2) in the north. Receiver spacing averaged over the length of the line was 0.85 km. Receivers on the north half of the profile sat on outcropping Cretaceous rocks. Receivers in the south were located on the Tertiary sediments. Starting in the north, from SP 2, the profile trends ESE then turns SW, passing obliquely through a band of NS-trending faults. The line then trends SE from 11 to 20 km running parallel to the Greenville fault zone. This portion of the line crosses the mapped trace of the fault twice, with the receivers laying in the fault zone. From 20 to 33 km, the line runs east, parallel to fold axes, crossing the Corral Hollow and Carnegie faults. South of SP 1, the line turns SE and runs parallel to and east of the Tesla fault. A plot of the mid-points between each shot and its receivers shows the approximate locations at which the rays turned, an indication of the area being sampled at depth (Figure 4). Zones of mid-point overlap from SP 1 and SP 2 represent the area of true reversed coverage.

A reduced travel-time plot of the data from SP 1 along the strike profile is shown in the center panel of Figure 3. The reducing velocity is 6 km/sec. Below the data

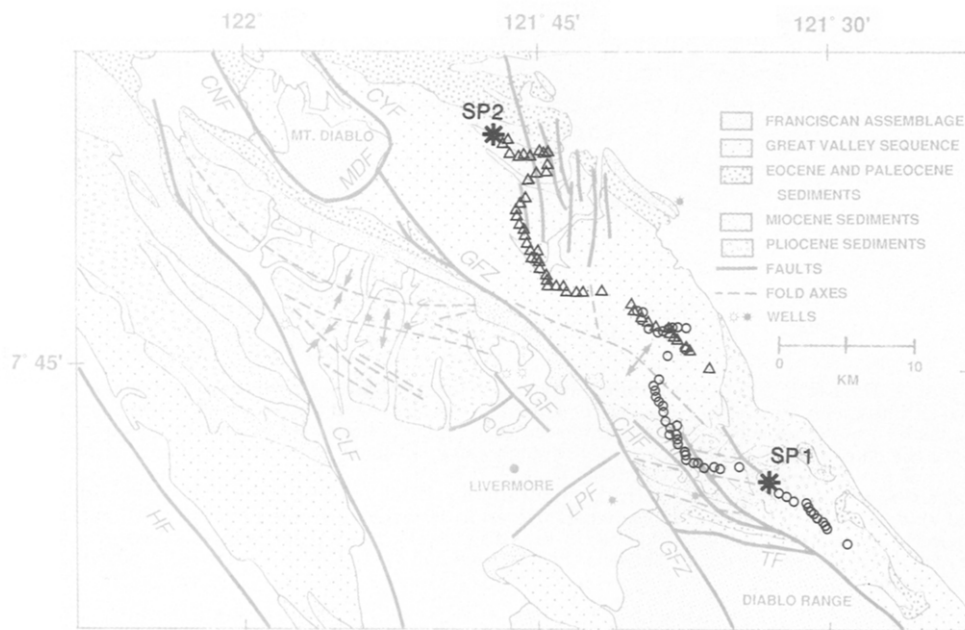


FIG. 4. Map of mid-points for SP 1 and SP 2 along the strike profile. Triangles are mid-points between SP 2 and receivers along the strike profile. The circles are the mid-points from SP 1. These points represent the approximate locations where the rays turn at depth, and show which part of the crust is being illuminated. Because of the receiver geometry, the turning points do not fall along a straight line. The zone of overlap between the mid-points from SP 2 and SP 1 show the area of reverse coverage, where rays from both shots traveled through the same part of the crust. The deepest interface in the model (top of the 5.5 km/sec layer) is well-constrained by the triplication seen in SP 2, and by the reverse coverage from SP 1. Abbreviations are the same as in Figure 1.

is the raytrace model derived from analysis of travel times and amplitudes. The raytrace models are plotted in depth, with sea level equal to 0.5 km depth in the model. Topography was included in each model. Rays were traced through each layer to receiver positions corresponding to the field receiver locations. In this figure, only rays that arrive as first arrivals are shown in order to reduce clutter on the plot. The ray diagram shows which part of the structure is being illuminated along the line. The complete travel-time curve, including both wide-angle reflections and refractions, is superimposed on the data. Synthetic seismograms are plotted above the data.

The strike profile model has a thin (0 to 650 m) upper layer of sediments with velocities ranging from 2.1 to 3.0 km/sec (Figure 3). These velocities were determined primarily by fitting the arrivals south of SP 1, and then extrapolating the layering north. This upper layer pinches out to the north at 15 km where the contact between Cretaceous and Tertiary rocks outcrops. The second layer in the model is 650 to 1,300 m thick with velocities of 3.5 to 3.6 km/sec. Velocities in this layer are primarily determined by the first arrivals from SP 2 (Figure 5). The other prominent shallow feature on this line is a low-velocity wedge modeled as extending horizontally from 1.5 to 10.5 km in the model, with a maximum depth of 0.6 km. The geometry of the wedge is constrained by the travel-time delay on traces between 2 to 9 km on SP 2. A velocity of 2.1 km/sec was assumed for the material in the wedge. The wedge must be a shallow feature, since the first arrivals at longer offsets to the south of the wedge (11 to 16 km) have almost zero intercept time, requiring that they turn at a shallow depth and pass beneath the low-velocity wedge undisturbed.

The third layer is modeled as being 2 to 4 km thick with a velocity of 4.0 to 4.2 km/sec. The velocity and dip of the top of this layer were determined from reversed arrivals from SP 1 and SP 2. The interface between the 3.5 to 3.6 km/sec layer and the 4.0 to 4.2 km/sec layer flattens beneath SP 1. Rays refracted below this interface occur as first arrivals south of SP 1, constraining the depth to the horizon. A thin layer (0.5 km) with a mild velocity inversion was included near the top of this layer in the model to account for the fall-off in amplitudes seen at 17 to 22 km from SP 2. A drop in velocity from 4.0 to 3.95 km/sec was enough to generate the observed fall-off in amplitude.

The deepest layer in the model has a velocity of 5.5 to 5.8 km/sec and occurs at a depth of 4.0 to 5.5 km. This is one of the best-constrained parts of the model because rays from both shots turn in the same part of the model. This is the zone of mid-point overlap shown in Figure 4. The dip of the layer is approximately  $5^\circ$  to the north beneath the reversed part of the line, but like the layer above, it flattens beneath SP 1. If the interface continued to shallow to the south, rays refracted along it would appear as first arrivals on the receivers south of SP 1. This is not seen in the data. The data to the south of SP 1 require that this interface be at least 4 km deep. The triplication associated with the reflections and refractions from this interface are a prominent feature on the record for SP 2. No near-offset reflections are observed in the data; therefore, the boundary between the layers is modeled as a 0.4-km-thick gradient zone, with velocities increasing from 4.2 to 5.5 km/sec within this zone. The relative amplitudes between the first arrivals and the wide-angle reflections are well-matched in the synthetic data. Arrivals from the deepest layer at the far offsets of SP 1 (0 to 5 km horizontal distance in the model) are delayed in time by travel through the low-velocity wedge at the surface.

*Geologic interpretation of strike profile.* The first two layers and the wedge material all outcrop at the surface. The shallow layer (2.1 to 3.0 km/sec) which pinches out

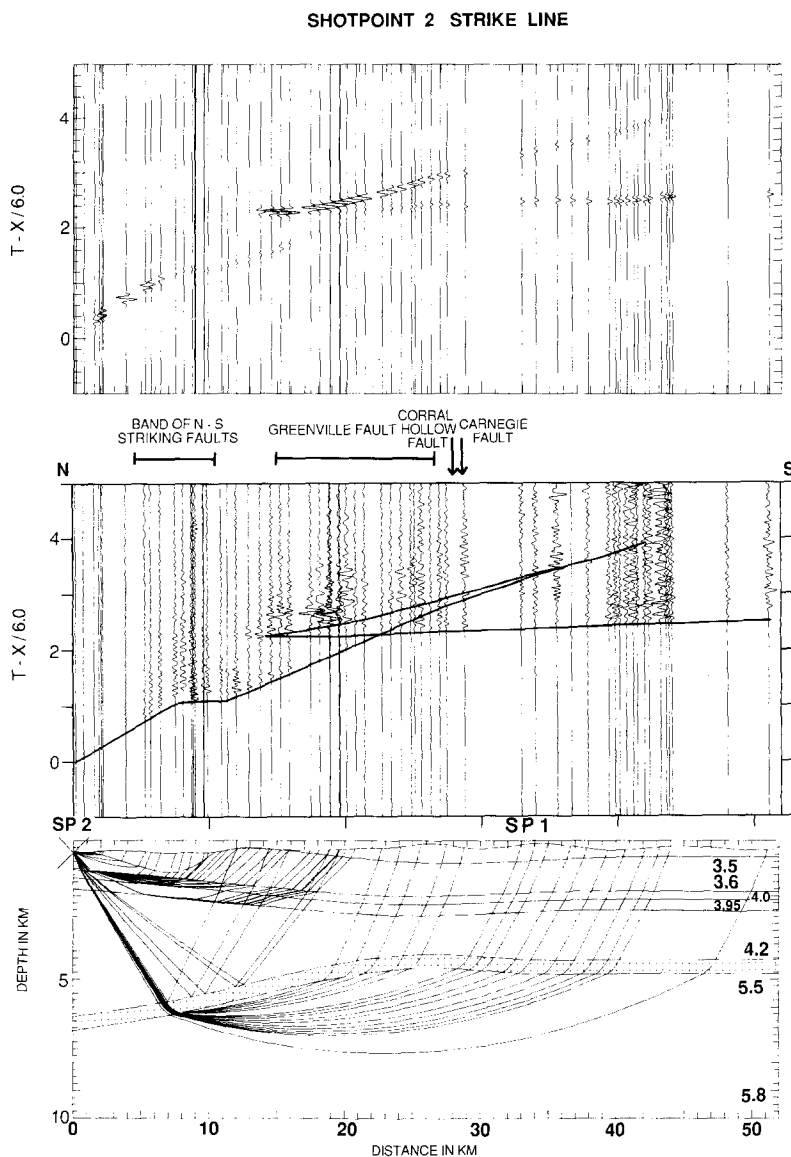


FIG. 5. Data, raytrace, and synthetic seismogram from SP 2, for the strike line. The low-velocity wedge is constrained by the travel-time delay on traces from 2 to 9 km and by the early arrivals from 11 to 17 km. The slight velocity inversion within the middle layer was included to account for the drop-off in amplitude between 17 and 22 km.

to the north corresponds to the predominantly Miocene outcrops on the south end of the line in the Corral Hollow area. This layer must pinch out to the north to accommodate the first arrivals from SP 2. The 3.5 to 3.6 km/sec layer coincides with outcrops of Cretaceous sediments of the Great Valley sequence on the north end of the line. Wells drilled near the profile have encountered up to 1,500 m of Neogene sedimentary rocks. Given that the structure is complex on the south end of the line east of the Greenville fault, and that the Cretaceous/Tertiary contact here is an unconformity, there is no reason to suspect that the boundary between Tertiary and Cretaceous rocks would follow a uniform interface. The interface between the two layers in the velocity model represents a change in velocity gradient



within the sedimentary section, rather than a stratigraphic or structural boundary. Sediments first increase in velocity rapidly with depth and then increase more slowly. Since the upper layer pinches out to the north, the gradient is not simply related to depth of burial. The low-velocity wedge at the surface corresponds to a zone of north-south trending faults. It could also be related to unconsolidated sediments associated with local drainage systems cutting through the Cretaceous rocks (Figure 1).

The 4.0 to 4.2 km/sec layer is interpreted to be the Cretaceous Great Valley sequence. Cretaceous rocks are by far the most prevalent rocks exposed at the surface east of the Greenville fault. To the east in the Central Valley, similar seismic velocities are found for a 3 to 5-km-thick layer of the Great Valley sequence at a similar depth (Colburn and Mooney, 1986; Holbrook and Mooney, 1987). Based on the seismic velocity, we infer that the deeper 5.5 to 5.8 km/sec layer is the Franciscan assemblage. Similar velocities are associated with Franciscan rocks in the Diablo Range (Walter and Mooney, 1982). Although seismic velocity alone cannot be used to identify Franciscan rocks, large masses of Franciscan rocks outcrop to the south and presumably lay at depth beneath the Great Valley sequence. A velocity of 5.5 km/sec could also correspond to serpentinites or the upper layers of oceanic crust (Christensen, 1978; Nichols *et al.*, 1980). Thus, this interface could also be interpreted as the boundary between the Great Valley sequence and altered oceanic crust or a buried remnant of the Coast Range thrust.

*Dip profile.* The WNW-ESE dip profile runs obliquely across the Livermore basin. Stations were laid out over 70 km, with an average station spacing of 1.23 km. There were 2 shotpoints along this profile, SP 1 in the east and SP 3 in the west (Figure 2). SP 1 is in the same location for both the strike and dip line, and the receivers east of the Greenville fault are also the same for both profiles. The same structure is being seen by both profiles SE of the Greenville fault. All stations on the dip profile sit on Tertiary sedimentary rocks. There is no outcropping Franciscan assemblage along the line. The line starts in the west with receivers from 0 to 16 km laid out toward the SE (Figure 2), and then turns east and crosses the Calaveras fault. From 20 to 25 km, the line runs north, trending perpendicular to the anticline-syncline fold axes of Livermore basin. From 25 to 35 km, the line runs roughly parallel to local structure, crossing a series of synclines and anticlines. At 35 km, the line crosses two buried faults. From 40 to 45 km, the profile trends SE within the Greenville fault zone. Like the strike profile, this line is crooked, and the mid-points do not fall along a straight line (Figure 6).

The data from SP 1 along the dip profile are shown in Figure 7. The model on the east end of the dip line is the same as that found on the strike line. West of the Greenville fault, the model is based on the data from shotpoint 3 (SP 3) (Figure 8). The data from SP 3 were modeled as a split spread, assuming plane-dipping layers. The model has three layers, the first, 800 to 1,000 m thick, has velocities increasing from 2.2 to 2.7 km/sec. The middle layer thickens to the east and has a velocity of 3.0 to 3.1 km/sec. This is underlain at depths of 2 to 4 km by a layer with velocities from 4.9 to 5.1 km/sec. The top of this layer dips east at approximately 3°. The control on velocity and dip come from the receivers within 12 km on either side of SP 3. The raytrace diagram indicates there is good control on the model from 8 to 34 km. Station spacing over this portion of the line was 0.8 km, denser than the average along the line. Beyond 34 km, the arrivals from SP 3 are extremely poor. The arrivals are weak from 34 to 38 km, and beyond 38 km they appear incoherent. Between 34 km and the Greenville fault zone, the model is unconstrained. The

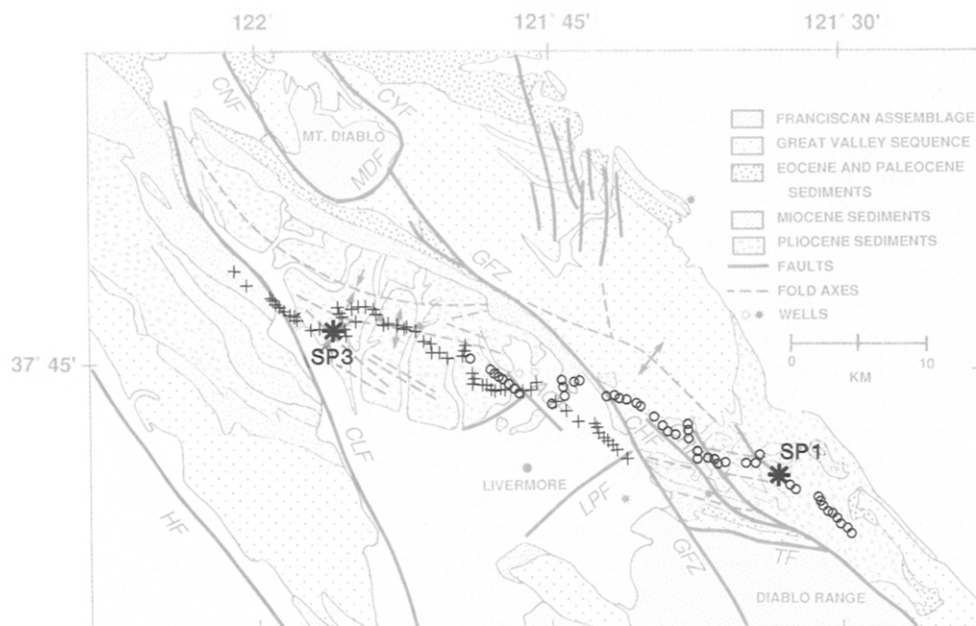


FIG. 6. Map of mid-points for SP 1 and SP 3, dip profile. Crosses are mid-points between SP 3 and receivers, and circles are the mid-points from SP 1. The zone of overlap, where circles and crosses coincide, shows area of reverse coverage. All of the mid-points from SP 3 occur west of the Greenville fault. The sinuous path of the image points illustrates that modeling this profile as two-dimensional is only an approximation. Abbreviations are the same as in Figure 1.

Calaveras fault crosses the profile approximately 4 km west of SP 3. Refracted arrivals crossing the fault appear continuous. The Calaveras fault does not appear to disrupt arrivals which pass through it, unlike the Greenville fault. Either the velocity structure on both sides of this fault is similar or there is no low-velocity zone associated with the Calaveras fault here.

There are several factors which may contribute to the overall degradation of the data on SP 3 beyond 34 km. The line of receivers at this point turns SE away from being aligned parallel to structure, to being transverse to structure. The spacing of fold axes along this part of the line is 1 to 2 km (Figure 2), and station spacing averages 1.23 km. Energy arriving at adjacent receivers may have followed different ray paths through the folded structure so that arrivals at the surface appear incoherent. In addition, at this distance, the line crosses the inferred location of the buried ancestral Greenville fault. Arrivals at stations in this area from SP 1 are also disrupted.

There are coherent arrivals at a few receivers at distances of 20 to 28 km on SP 1. These arrivals presumably followed ray paths which turned below the fault and are used to infer the 5.5 km/sec interface at depth west of the Greenville fault zone. The 5.5 km/sec layer east of the Greenville fault is constrained by the reverse coverage of the strike profile coincident with the eastern portion of the dip profile.

There are many exploratory wells drilled on structures in the Pliocene outcrops of the Tassajara Hills (California Division of Oil and Gas, 1980). The deepest of these, Cities Services, Gumpert #1, located at 22 km along the dip profile, extends 5,315 m (17,432 ft), bottoming in Miocene sediments. Another well, Humble Oil, Hans Nielsen #1, bottomed in Neogene sediments at 4,033 m (13,230 ft) and is located at 27 km along the profile. A third well at 17 km, Butte-Weideman #1,

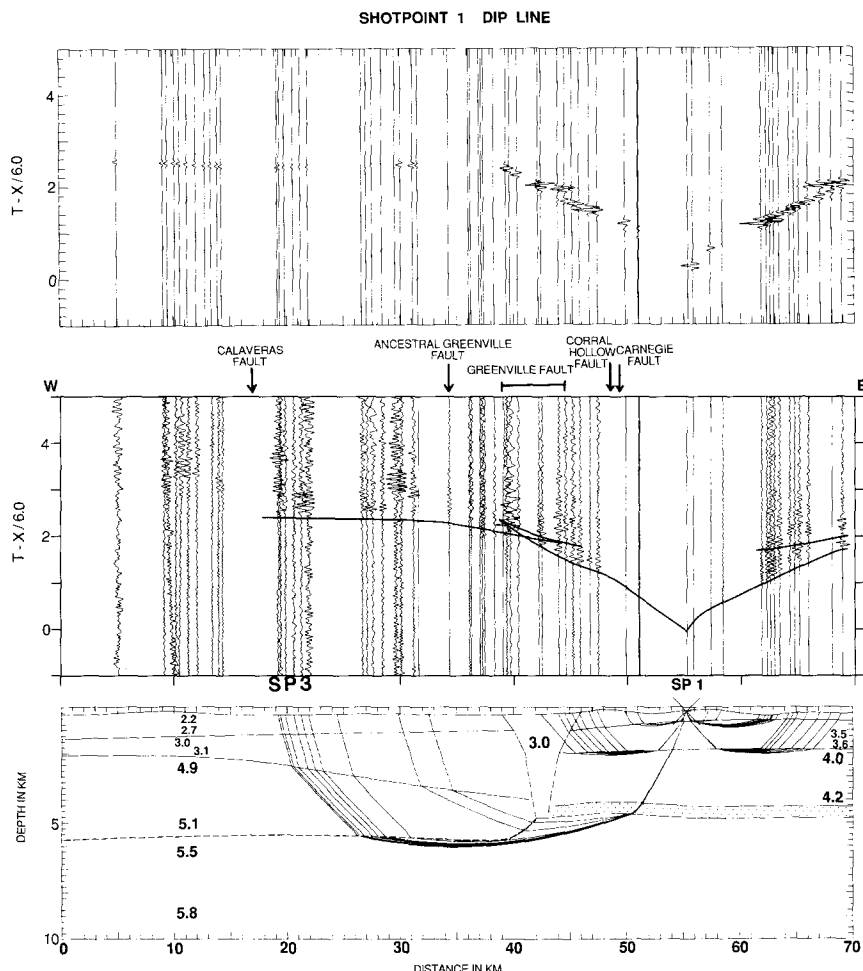


FIG. 7. Data, raytrace, and synthetic seismogram from SP 1, dip profile. Intersection of major faults with the receivers is shown above the data. The model east of the Greenville fault is the same as the strike profile (Figure 3). Model west of the Greenville fault is based on the data from SP 3. The 5.5 km/sec interface west of the fault is inferred from a coherent arrival at a few receivers from rays which turn below the fault zone.

drilled upper Miocene sediments at a total depth of 2,834 m (9,297 ft). All of the wells drilled in the Tassajara Hills penetrated only Pliocene and Miocene sediments at depth. Sonic logs from only two of the wells (Gumpert #1 and Hans Nielsen #1) are available for this part of the Livermore Valley (Figure 9). The overall velocity structure from the sonic logs is quite similar to that derived from the refraction data, although it is different in detail because it has finer vertical resolution. The sonic logs confirm the high velocities (4.84 and 5.08 km/sec) seen in the refraction data. The Hans Nielsen well shows a velocity inversion below 3.5 km, after reaching a velocity of 4.84 km/sec at 3.3 km depth, the velocity drops to 4.06 km/sec. Unfortunately, at this depth, the Gumpert #1 well had a break in the log. Logging was resumed at 4,570 m (15,000 ft), with velocities of 4.69 km/sec. The highest velocity logged in either well was 5.08 km/sec at 4,948 m (16,320 ft).

An alternate velocity model for SP 3 was constructed based on the sonic velocities recorded in the two wells (Figure 10). The differences introduced by sonic log information are: (1) the velocity structure within the 3.0 to 3.1 km/sec layer is

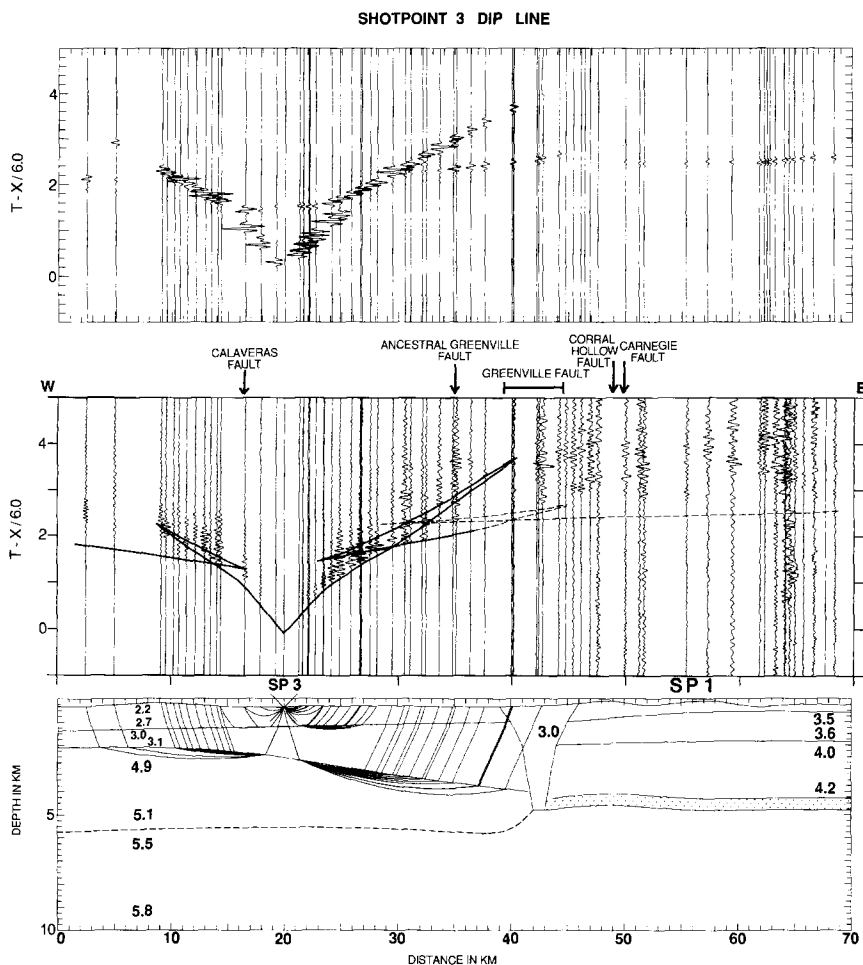


FIG. 8. Data, raytrace, and synthetic seismogram from SP 3. Between 8 and 34 km, the velocity model is well-constrained by the arrivals on both sides of the shot. Beyond 34 km, the model is unconstrained west of the Greenville fault. First arrivals from the deepest layer (5.5 km/sec) are not observed in the data. The dashed line superimposed on the data represents the 5.5 km/sec arrival predicted by the model.

broken into several layers which pinch out to the west; (2) the velocity of the 4.9 to 5.1 km/sec layer shown if Figure 8 was changed to 4.8 to 5.0 km/sec to match the sonic logs; (3) the top of this layer is deeper east of SP 3 in the alternate model—3.5 km versus 3.0 km; and (4) the velocity inversion beneath the 4.8 to 5.0 km/sec layer was included. This velocity inversion provides an alternate explanation for the loss of amplitude in arrivals from SP 3 beyond 34 km. In order for the first arrivals west of SP 3 to be accurately modeled, the intermediate layers must pinch out to the west, and the 4.8 to 5.0 km/sec interface must shallow to the west. The Greenville fault zone was left off the alternate model because we were interested in modeling the basin structure west of the fault. The layers in the alternate model are relatively thin, and the refraction data do not resolve this finer structure well; however, the alternate model fits the refraction data and conforms to the well log information. Reflections from the bottom of the 4.8 to 5.0 km/sec layer fit later arrivals in the refraction data, particularly east of SP 3. We prefer the alternate model.

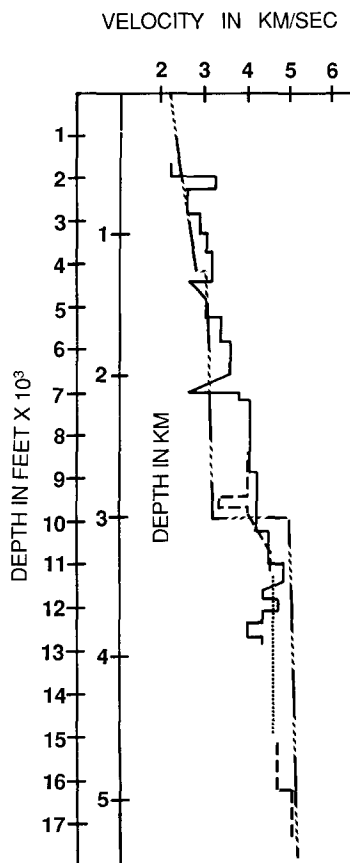


FIG. 9. Well logs through Livermore basin sediments. Solid line is sonic log from Hans Nielsen #1, and dashed line is from Gumpert #1. The dotted line represents a break in logging in the Gumpert #1 well. Both wells penetrated only Pliocene and Miocene rocks. Dot-dashed line is the velocity-depth model derived solely from the refraction data. This refraction model was altered to include the finer structure found in the sonic logs (see Figure 10).

*Geologic interpretation of the dip profile.* All of the layers above the 5.5 km/sec layer in the velocity model from SP 3 (Figures 8 and 10) west of the Greenville fault, correspond to Neogene sedimentary rocks, including the 4.9 to 5.1 km/sec layer. The 3.1 to 4.9 km/sec velocity interface within the sedimentary section does not correspond to a sedimentary interface between formations. Wells located along the dip profile at 34 and 36 km penetrated upper Cretaceous sediments at depths of 2,920 m (9,580 ft) and 2,073 m (6,800 ft), respectively, within the 3.0 to 3.1 km/sec layer of the dip profile. Thus, the velocity interface does not correspond to the unconformity separating Neogene from pre-Neogene sediments. Formations within the basin have complex stratigraphic and structural relations, and boundaries between them would not be likely to follow such a uniform interface.

The 3.1 to 4.9 km/sec velocity interface probably corresponds to a diagenetic boundary related to previous deeper burial and cementation of the sediments. Although the Miocene Monterey formation is present in the basin, it is a silty facies of the Monterey and does not appear to exhibit the diagenetic characteristics associated with the siliceous facies of the Monterey found elsewhere in California (Pisciotta and Garrison, 1981). The lower layer in the model with velocities of 5.5 to 5.8 km/sec west of the Greenville fault may be Franciscan rocks underlying the

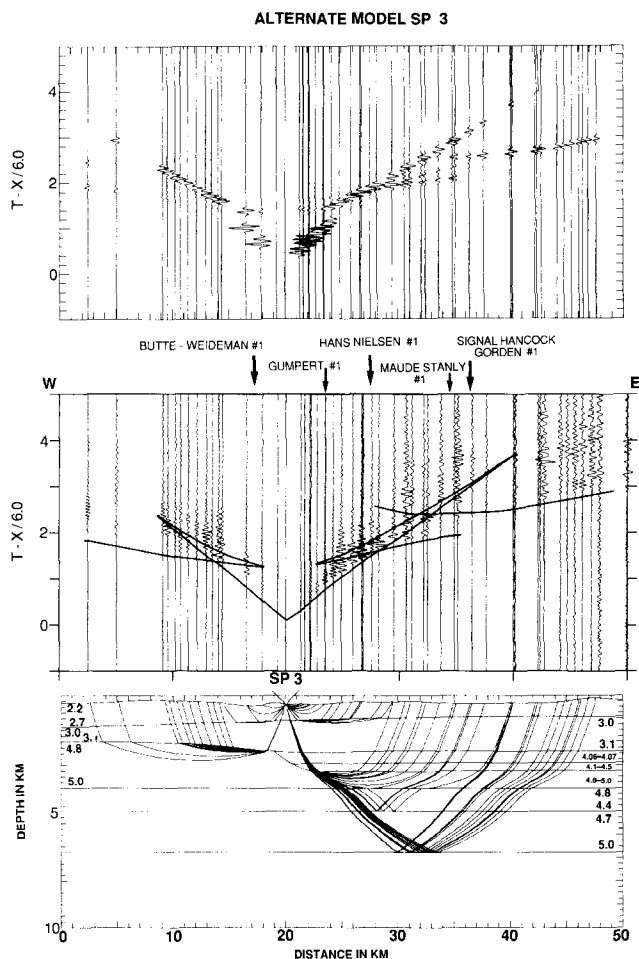


FIG. 10. Alternate model for SP 3 based on sonic logs in Figure 9. Locations of wells along the line are plotted directly above the data. Butte-Weideman, Gumpert, and Hans Nielsen drilled through Miocene and Pliocene rocks. Maude Stanly and Signal Hancock drilled through Cretaceous rocks.

sedimentary basin. The layer is inferred from the continuous arrivals on SP 1 at 20 to 28 km in the model. No arrivals from this layer are observed in the data from SP 3. This may be because all of the rays from SP 3 turn west of the Greenville fault, passing through it, while arrivals at far offsets from SP 1 pass beneath the Greenville fault (Figures 6 and 7).

From 40 to 45 km, the line crosses and trends parallel to the Greenville fault zone, disrupting arrivals from SP 3. Data from SP 1 along the dip profile also appear to be disrupted by passage through the fault zone, although there are a few coherent arrivals at the far offsets from SP 1. This portion of the line corresponds to the area of mid-point overlap from SP 1 and SP 3 (Figure 6). Since the data from both shotpoints are severely degraded, the shots do not truly reverse each other. The Greenville fault zone is modeled here as a wedge-shaped feature. The velocity, shape, and extent of a shear zone associated with this fault is not constrained by the data; however, similar structures have been modeled on refraction profiles crossing other strike-slip faults in the California Coast Ranges (Mooney and Colburn, 1985). Ray paths which are transverse to the fault zone are disrupted by travel through it, and the velocity structure is different on either side of the fault.

The Greenville fault zone represents a major boundary in the upper crust in the Livermore Valley area.

### DISCUSSION AND SUMMARY

The overall velocity structure presented here for the two Livermore refraction profiles is similar to the shallow portions (2 to 7 km) of velocity models found on two nearby strike profiles: one located to the east in the Central Valley (Colburn and Mooney, 1986), and the other, a regional line located through the Diablo Range extending north through Livermore Valley (Walter and Mooney, 1982). The velocity structure presented here is also generally similar to Taylor and Schiener's (1982) velocity model which was determined from inversion of earthquake and shot data for the same region. Our preferred velocity models for the Livermore Valley area are shown in Figure 11, along with comparisons to the studies cited above. The 4.9 and 5.5 km/sec refractors seen in the data presented here were also identified on the regional refraction line through Livermore Valley, but were interpreted as Franciscan rocks. In the local earthquake inversion, a 5.0 to 5.7 km/sec layer was found at depths of 5 to 8 km, and interpreted as possible Great Valley sequence or Franciscan assemblage rocks. The well data in the basin show that the upper interface is within the sedimentary basin fill and is not the boundary between sediments and Franciscan rocks. The velocity of these sediments is very high in

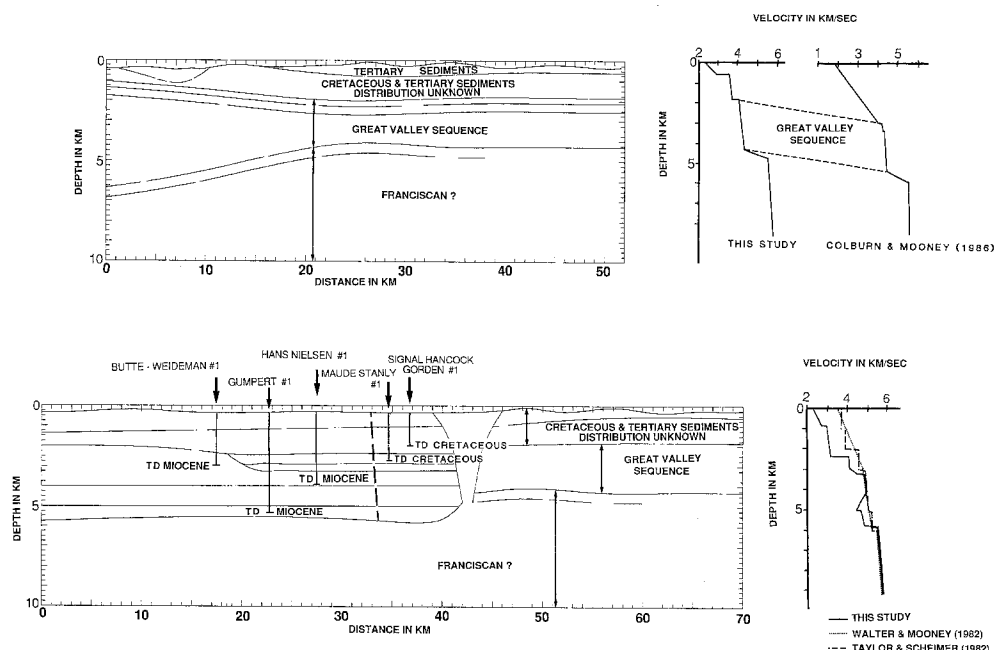


FIG. 11. Final models with geologic interpretation. Velocity-depth profiles for the Livermore area strike line and for a strike profile 15 km east in the Central Valley (Colburn and Mooney, 1986) show similar layer thicknesses and velocities in the Great Valley sequence east of the Greenville fault. Well locations and the age of sediments found at the bottom of each well are superimposed on the final model for the dip profile through the Livermore Valley. The Ancestral Greenville fault (dashed line) separates wells which penetrate Cretaceous rocks from wells which penetrate only Pliocene and Miocene sediments. The model is inferred between 34 km and the Greenville fault. Layering constrained by first arrivals 12 km on either side of SP 3 were extrapolated to the fault. The well data show that the upper two layers contain sediments of both Tertiary and Cretaceous age. The layering shown in the model represents velocity structure and not stratigraphic layering. Velocity versus depth profiles are shown from Taylor and Schiener (1982) and Walter and Mooney (1982) for comparison with the velocity structure found in this study.

comparison to velocities of the Cretaceous sediments east of the Greenville fault. The clearly different velocity structures found within the sediments on either side of the Greenville fault implies a different tectonic history in terms of sediment burial, diagenesis, and uplift for the areas on either side of the fault. In contrast, this refraction profile exhibits little change in velocity structure across the Calaveras fault to 2.5 km depth. Below 2.5 km, the velocity structure on either side of the fault is different, and is the only seismic expression of the fault at this location. A low-velocity wedge is associated with the Calaveras fault elsewhere (Mooney and Colburn, 1985). The velocity model interpreted along the dip profile is an average velocity structure. Given the structural complexity of the Livermore basin, the receiver spacing, and the geometry of the line, the dip profile cannot adequately resolve any of the fine details of basin structure. Basement structure beneath the sedimentary basin fill cannot be constrained because of the lack of data at the far offsets of SP 3. The preferred model for SP 3 utilizing information from the sonic logs provides an interesting comparison to the model derived solely from the refraction data and is a closer match to the recorded data. It also illustrates the nonuniqueness of refraction interpretation, especially in the absence of reversing data.

The lower layer inferred here along the dip profile (5.5 to 5.8 km/sec) is also observed on the regional reversed refraction profile (Walter and Mooney, 1982). This arrival may be from the boundary between the Livermore basin fill and the underlying Franciscan assemblage. If this layer is the Franciscan Assemblage, then Cretaceous sediments appear to be absent directly beneath the Livermore basin. Any previously deposited Cretaceous sediments may have been eroded prior to deposition of the Neogene section; or, alternatively, the Neogene sediments may have been deposited directly above the Franciscan basement during Neogene wrench faulting. A sonic log from a well just west of the Greenville fault which penetrated the Franciscan is plotted in Figure 12, along with sonic logs from two wells which drilled through Cretaceous rocks. The three wells extend to depths of 1 to 2 km. The sonic logs in the Cretaceous sediments reach velocities of 3.8 km/sec and show several velocity inversions ranging from 65 to 300 m thick. The velocity profile for the well which drilled through the Franciscan has an initial velocity of 4.06 km/sec at 620 m, where it first penetrates the Franciscan. The velocity jumps to 5.54 km/sec at 770 m and then drops to 5.08 km/sec at 810 m. It maintains this velocity to the bottom of the well at 1,036 m. Berry (1973) suggests that an inverse velocity gradient should be associated with the Franciscan assemblage because where it is penetrated by wells it is often overpressured. This one shallow sonic log is not proof of this phenomenon, but if this feature were found in a significant number of logs, it would be important for the correct identification of Franciscan rocks and for differentiating them from other lithologies with similar velocities. The two profiles presented here lack the station density required to look at velocity gradients within the modeled Franciscan layers. Longer lines with greater receiver and shot density should be able to do so.

A relatively simple velocity structure satisfied the refraction data along the strike profile despite the potential complexities from the crooked line geometry and geologic structure. The velocity inversion within the 4.0 to 4.2 layer is reasonable, given the variability in velocity observed in the sonic logs through the Cretaceous rocks (Figure 12). The velocity model proposed for the strike profile is similar to that found from 2 to 7 km depth along a strike profile located approximately 25 km to the east along the western margin of the Central Valley. An interface between a



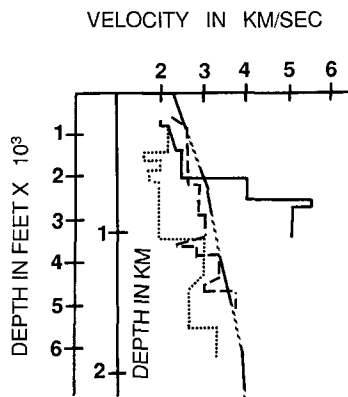


FIG. 12. Sonic logs through Cretaceous and Franciscan rocks. Dotted line and dashed line represent the Coelho & Sons #1, and Mulqueeney #1 wells, respectively. These wells drilled through Cretaceous rocks. Velocities in the sonic logs show a great deal of fluctuation. Solid line is from the Wisner #1 well which penetrated Franciscan rocks at 620 m. The velocities logged in this well show a rapid increase, followed by a decrease after penetrating the Franciscan assemblage. Dot-dashed line is the velocity-depth model derived from the refraction data for Cretaceous rocks east of the Greenville fault zone.

4.25 and a 5.5 km/sec layer identified in this depth range was interpreted as the boundary between the Great Valley sequence and underlying rocks (Colburn and Mooney, 1986). We interpret the boundary between the 4.0 to 4.2 km/sec layer and the 5.5 km/sec layer to be the Great Valley sequence/Franciscan boundary, although we emphasize that velocity alone cannot be used to identify Franciscan rocks. This boundary has an apparent dip of  $5^\circ$  to the north and occurs below 4.0 km depth. If this contact is a fault, it is probably not connected with the present-day Greenville fault, as this would require dips of  $45^\circ$  to  $63^\circ$ . It may represent a previous thrust fault between forearc basin and accretionary complex rocks (i.e., the Coast Range Thrust) which has been cut by later strike-slip motion along the Greenville fault. The Greenville fault has no apparent expression along the strike profile because all of the mid-points along the profile are well east of the fault (Figure 4).

We attribute the differences in amplitudes between the field data and the synthetics to be due to a combination of factors. The crooked line geometry and rapid structural variation can produce amplitude fluctuations which we cannot accurately model. In addition, we have not included the effects of anelastic attenuation. Amplitudes on the strike line, where structural variation is presumably less, are modeled accurately from both shotpoints. Arrivals in the triplication at 20 km (SP 2) and 40 km (SP 1) are well-modeled in size if not in exact detail. Amplitudes on the dip line are reasonably well-matched in the preferred model, although near-offset traces in both models appear with greater amplitudes than those observed. This is probably due to low  $Q$  in the upper sedimentary layers.

The shallow crustal models presented here for the Livermore basin are consistent with the proposed wrench fault basin models (Springer, 1983; Aydin and Page, 1984). Livermore basin is filled with a thick sequence ( $>5$  km) of Neogene sediments and is bounded by major strike-slip faults. The high velocity (5.0 km/sec) associated with the basin sediments suggest deep burial followed by uplift. This high velocity is in contrast to the Cretaceous Great Valley sequence sediments found east of the Greenville fault, which were also previously buried deeper, but have a maximum velocity of only 4.2 km/sec. The Greenville fault zone forms a major upper crustal boundary in the Livermore area. Arrivals in the refraction data which traveled along

paths parallel to the Greenville fault zone do not appear to be disrupted by the fault zone, whereas energy passing through the fault zone is severely attenuated. The existence of the ancestral Greenville fault is inferred by the data recorded along the dip profile. Energy arriving at receivers above the mapped location of the fault is degraded along both SP 1 and SP 3. This could be due to the juxtaposition across this fault of high-velocity sediments associated with the Livermore basin and the lower velocity sediments originally deposited east of the basin. Near-offset arrivals west of SP 3 which pass through the Calaveras fault zone are continuous. Although the Calaveras fault is a major strike-slip fault, there is no low-velocity wedge associated with the fault at this location.

## REFERENCES

- Atwater, T. (1970). Implications of plate tectonics for the Cenozoic tectonic evolution of western North America, *Geol. Soc. Am. Bull.* **81**, 3513–3535.
- Atwater, T. and P. Molnar (1973). Relative motion of the Pacific and North American plates deduced from sea-floor spreading in the Atlantic, Indian, and South Pacific Oceans, in *Proceedings of the Conference on Tectonic Problems of the San Andreas Fault System*, R. L. Kovach and A. Nur, Editors, Stanford University Publication of Geological Science, **13**, 136–148.
- Aydin, A. and B. M. Page (1984). Diverse Pliocene-Quaternary tectonics in a transform environment, San Francisco Bay Region, California, *Geol. Soc. Am. Bull.* **95**, 1303–1317.
- Bailey, E. H., W. D. Irwin, and D. L. Jones (1964). Franciscan and related rocks, and their significance in the geology of Western California, *Calif. Div. Mines Geol. Bull.* **183**, 177 pp.
- Bailey, E. H., M. C. Blake, and D. L. Jones (1970). Onland Mesozoic oceanic crust in the California Coast Ranges, *U.S. Geol. Surv., Profess Paper 700-C*, 70–81.
- Berry, F. A. (1973). High fluid potentials in California Coast Ranges and their tectonic significance, *Am. Assoc. Petrol. Geol. Bull.* **57**, 1219–1249.
- Blake, M. C., R. H. Campbell, T. W. Dibblee, D. G. Howell, T. H. Nilsen, W. R. Normark, J. C. Vedder, and E. A. Silver (1978). Neogene basin formation in relation to plate-tectonic evolution of San Andreas Fault system, California, *Am. Assoc. Petrol. Geol. Bull.* **62**, 344–372.
- California Division of Oil and Gas (1980). Oil and gas prospect wells drilled in California through 1980, California Division of Oil and Gas Publication TR01, Sacramento, California, 258 pp.
- Carpenter, D. W., J. J. Sweeny, P. W. Kasameyer, N. R. Burkhand, K. G. Knauss, and R. J. Shlemon (1984). Geology of the Lawrence Livermore National Laboratory site and adjacent areas, Lawrence Livermore National Laboratory UCRL-53316, 150 pp.
- Červený, V., I. A. Moltokov, and I. Psencik (1977). *Ray Method in Seismology*, University of Karlova, Prague, Czechoslovakia, 214 pp.
- Christensen, C. A. (1978). Ophiolites, seismic velocities and oceanic crustal structure, *Tectonophysics* **47**, 131–157.
- Colburn, R. H. and W. D. Mooney (1986). Two-dimensional velocity structure along the synclinal axis of the Great Valley, California, *Bull. Seism. Soc. Am.* **76**, 1305–1322.
- COSUNA (1984). Correlation of stratigraphic units of North America project, Central California Region, #686, American Association of Petroleum Geology, Tulsa, Oklahoma, 1 plate.
- Crowell, J. C. (1974). Origin of Late Cenozoic basins in southern California, in *Tectonics and Sedimentation*, Special Publication 22, W. R. Dickinson, Editor, SEPM, Los Angeles, California, 190–204.
- Dibblee, T. W. and R. L. Darrow (1981). Geology of the Northern Diablo Range and Livermore Valley area, in *Geology of the Central and Northern Diablo Range, California, Field Trip Guide 22*, V. Frizzell, Editor, Pacific Section of SEPM, Los Angeles, California, 77–84.
- Dickinson, W. R. (1976). Sedimentary basins developed during evolution of Mesozoic-Cenozoic arc-trench system in Western North America, *Can. J. Earth Sci.* **13**, 1268–1287.
- Dickinson, W. R. and D. R. Seely (1979). Structure and stratigraphy of forearc regions, *Am. Assoc. Petrol. Geol. Bull.* **63**, 2–31.
- Dickinson, W. R. and W. S. Snyder (1979). Geometry of triple junctions related to the San Andreas transform, *J. Geophys. Res.* **84**, 561–572.
- Ellsworth, W. L. and S. M. Marks (1980). Seismicity of the Livermore Valley, California region, 1969–1977, *U.S. Geol. Surv., Open-File Rept.* 80–515.
- Ernst, W. G. (1970). Tectonic contact between the Franciscan melange and the Great Valley sequence—Crustal expression of a late Mesozoic Benioff zone, *J. Geophys. Res.* **75**, 886–901.

- Graham, S. A., C. M. McCloy, M. Hitzman, R. Ward, and R. Turner (1984). Basin evolution during change from convergent to transform continental margin in Central California, *Am. Assoc. Petrol. Geol. Bull.* **68**, 233-249.
- Holbrook, W. S. and W. D. Mooney (1987). The crustal structure of the axis of the Great Valley, California, from seismic refraction data, *Tectonophysics* (in press).
- Ingersoll, R. V. (1982). Initiation and evolution of the Great Valley forearc basin of northern and central California, U. S. A., in *Trench-Forearc Geology*, Special Publication 10, J. K. Leggett, Editor, Geological Society of London, London, England, 459-467.
- McMechan, G. A. and W. D. Mooney (1980). Asymptotic ray theory and synthetic seismograms for laterally varying structure: theory and application to the Imperial Valley California, *Bull. Seism. Soc. Am.* **70**, 2021-2035.
- Minster, J. B. and T. H. Jordan, (1978). Present day plate motions, *J. Geophys. Res.* **83**, 5331-5354.
- Mooney, W. D. and R. H. Colburn (1985). A seismic refraction profile across the San Andreas, Sargent, and Calaveras faults, West-Central California, *Bull. Seism. Soc. Am.* **75**, 175-191.
- Nichols, J., N. Warren, B. P. Luyendyk, and P. Spudich (1980). Seismic velocity structure of the ophiolite at Point Sal, Southern California, determined from laboratory measurements, *Geophys. J. R. Astr. Soc.* **63**, 165-185.
- Page, B. M. (1966). Geology of the Coast Ranges of California, *Calif. Div. Mines Geol. Bull.* **190**, 255-276.
- Page, B. M. (1981). The southern Coast Ranges, in *The Geotectonic Development of California*, W. G. Ernst, Editor, Prentice-Hall, Englewood Cliffs, New Jersey, 330-417.
- Page, B. M. and D. C. Engebretson (1984). Correlation between the geologic record and computed plate motions for Central California, *Tectonics* **3**, 133-156.
- Pisciotta, K. A. and R. E. Garrison (1981). Lithofacies and depositional environments of the Monterey formation, California, in *The Monterey Formation and Related Siliceous Rocks of California*, R. E. Garrison and R. G. Douglas, Editors, Special Publication of the Pacific Section of SEPM, 97-122.
- Rodgers, D. A. (1980). Analysis of pull-apart basin development produced by en echelon strike-slip faults, in *Sedimentation in Oblique-Slip Mobile Zones*, P. F. Ballance and H. G. Reading, Editors, Special Publication of the International Association of Sedimentologists, **4**, 27-41.
- Springer, J. E. (1983). Structural analysis of the Southern Livermore basin, California, Lawrence Livermore National Laboratory UCID-19805, 178 pp.
- Sweeney, J. J. (1982). Magnitudes of slip along the Greenville fault in the Diablo Range and Corral Hollow areas, *Proceedings of the Conference on Earthquake Hazards in the Eastern San Francisco Bay Area*, 137-146.
- Taylor, S. R. and J. F. Scheimer (1982). *P*-velocity models and earthquake locations in the Livermore Valley region, California, *Bull. Seism. Soc. Am.* **72**, 1255-1275.
- Walter, A. W. and W. D. Mooney (1982). Crustal structure of the Diablo and Gabilan Ranges, Central California: a reinterpretation of existing data, *Bull. Seism. Soc. Am.* **72**, 1567-1590.

DEPARTMENT OF GEOLOGY AND GEOPHYSICS  
RICE UNIVERSITY  
P.O. BOX 1892  
HOUSTON, TEXAS 77251 (A.S.M., A.R.L.)

U.S. GEOLOGICAL SURVEY  
345 MIDDLEFIELD ROAD  
MS 977  
MENLO PARK, CALIFORNIA 94025 (W.D.M.)

Manuscript received 28 October 1986